Supplementary Figure Legends

Supplementary Figure S1: **CLIP revealed no interaction of *Snhg15* and EZH2 in CB cells.** RNA recovery for IgG and anti-EZH2 antibody CLIP samples in CB cells (N = 5 biological replicates). For all investigated amplicons, the recovery for EZH2 could not be statistically differentiated from the IgG-based pulldown. Whiskers of the box plots extend 1.5 times the interquartile range from the 25th and 75th percentiles (Tukey style) while outliers are represented by hollow dots. Significances were determined with two-tailed Student's *t*-test. ctrl-Fc: control Fc, efnA5-Fc: ephrinA5-Fc, CB: cerebellar granule, CLIP: UV cross-linking and immunoprecipitation.

Supplementary Figure S2: NCAM1 is implicated in the survival rate of low-grade glioma patients and its expression can be downregulated in murine cells via RNA silencing. (a) High expression levels of *NCAM1* are associated with increased patient survival in low-grade glioma. Survival analysis is based on clinical data and gene expression counts from tumor samples of lower grade glioma patients downloaded from BioPortal (http://www.cbioportal.org/study/clinicalData?id=lgg_tcga) and The Cancer Genome Atlas (TCGA), respectively. (b) Knockdown efficiency of the applied *Ncam1* siRNA (N = 3 biological replicates). Significances were determined with log-rank (a) and Wilcoxon-Mann-Whitney test (b). Significance levels: p value < 0.05 *; p value < 0.01 **; p value < 0.001 ***. ctrl: control. LGG: low-grade glioma. siR: siRNA.

Supplementary Figure S3: Migratory analysis of CB cells upon stimulation with ephrinA5-Fc and downregulation of *EphA2*. The motility of CB cells was reduced upon stimulation with ephrinA5-Fc. (a) Temporal color-coded migratory distance over 20 h of imaging. The starting point of migration for each cell is shown in dark blue and the end point in white. (b) Quantitative analysis of average migratory speed (n = 268 for ctrl siR + ctrl-Fc, n = 244 for ctrl siR + efnA5-Fc, n = 273 for *EphA2* siR + ctrl-Fc, n = 238 for *EphA2* siR + efnA5-Fc, N = 3 biological replicates). (c) Knockdown efficiency of the applied *EphA2*-siRNA (N = 3 biological replicates). Significances were determined with one-way ANOVA (b) and Wilcoxon-Mann-Whitney test (c). Significance levels: p value < 0.05 *; p value < 0.01 **; p value < 0.001 ***. Scale bar: 100 µm. ctrl: control. efnA5: ephrinA5. siR: siRNA.

Supplementary Figure S4: Native ChIP reveals no changes in DNMT1 association and histone methylation signatures within the proximity of a *cis*-regulatory element of *Adamts14* and the putative *Snhg15* binding sites. (a) Genomic regions targeted by the primers are shown in turquoise. The promoter is shown in dark blue, candidate cis-regulatory elements in red, and putative *Snhg15* binding sites in pink. (b-c) ChIP-qPCR analysis with anti-DNMT1 and anti-H3K27me3 antibodies for the promoter region of *Adamts14* normalized against the input material and IgG (N = 3 biological replicates for *P1* (b), N = 4 biological replicates for *P2* (c)). Significances were determined with two-tailed Student's *t*-test. Significance levels: p value < 0.05 *; p value < 0.01 **; p value < 0.001 ***. ctrl: control. efnA5: ephrinA5.

Supplementary Figure S5: Root mean square deviation (RMSD) plot for *Ncam1*, *Ncam1*-ext, *Adamts14*-1 and *Adamts14*-2 taken over the entire trajectory of 600 ns for (a) the RNA strand of the triple helix and (b) the DNA double helix.

Supplementary Figure S6: Comparison of energy contributions between the two *Adamts14* models (*Adamts14*-1 and *Adamts14*-2). The hydrogen bond energies between individual residues at the same base pair level (i) were calculated by taking the sum of Lennard-Jones (LJ) and Coulomb (CB) short range interaction energies. The cross energies were calculated for a base pair level (i) by considering the sum of LJ and CB short range interaction energies of (i)th residue in chain B with (i+1)th and (i-1)th residue in chain A and C. The stacking energies were calculated for a base pair step level by considering the sum of LJ and CB short range interaction energies of (i)th and (i+1)th residues in chain A, B and C. The total plot shows the sum of the contribution of individual energies at the (i)th base pair level. In all calculations the energy contributions involving terminal residues were not included to avoid discrepancy in the number of terms that contribute.

Supplementary Figure S7: Comparison of energy contributions between the two *Ncam1* models (*Ncam1* and *Ncam1*-ext). The hydrogen bond energies between individual residues at the same base pair level (i) were calculated by taking the sum of Lennard-Jones (LJ) and Coulomb (CB) short range interaction energies. The cross energies were calculated for a base pair level (i) by considering the sum of LJ and CB short range interaction energies of (i)th residue in chain B with (i+1)th and (i-1)th residue in chain A and C. The stacking energies were calculated for a base pair step level by considering the sum of LJ and CB short range interaction energies of the (i)th and (i+1)th residue in chain A, B and C. The total plot shows the sum of the contribution of individual energies at the (i)th base pair level. In all calculations the energy contributions involving terminal residues were not included to avoid discrepancy in the number of terms that contribute.

Supplementary Figure S8: Display of all hydrogen bonded interactions of the RNA that occur with frequency >1% in the (a) *Adamts14*-1 and (b) *Ncam1*-ext simulation. For clarity the purine DNA strand was drawn above, and the pyrimidine DNA strand below the RNA. H-bonds between the two DNA strands as well as within individual strands are omitted to focus on the H-bond patterns of the RNA strand. Occurrence is in “H-bond units”, i.e., an occurrence of >100% indicates that on average there exists more than one H-bond between the respective residues.

Supplementary Table S1: Sequences of applied primer pairs in (RT-)qPCR experiments.

Supplementary Table S2: Detailed sequences of the simulated systems (*Adamts14*-1, *Adamts14*-2*, Ncam1, Ncam1*-ext*)*. Pairing between DNA sequences (black) and RNA sequences (red) is predicted to form triple helixes for two binding sites in the *Adamts14* promoter and one binding site at the *Ncam1* promoter. 5’ and 3’ indicates the orientation of the DNA and RNA strands. “|” indicates base pairing following triple helix canonical code, while “*” indicates positions with a mismatch.

Supplementary Table S3. Differentially methylated sites in CB cells treated with ephrinA5-Fc. Table lists all sites/regions (DMS/DMRs) with an adjusted *p* value ≤ 0.05 (adj. *p*val). (From left to right) Target ID of the probe – locus identifier (cg=CpG) with numeric code (ID), intercept value (intercept), F-value (f), p-value (pval), q-value (qval), mean coefficient of Control-FC samples (mean.coeff.Ctrl.FC), mean coefficient of Efna5-FC samples (mean.coeff.efna5.FC), direction of methylation (Methylation), fold

change (FC), color of the channel used for probe signal detection (Color_channel), number of the chromosome of the probe location (chr), sequence of the probe identified in the AddressA_ID column (AlleleA_ProbeSeq), sequence of the probe identified in the AddressB_ID column (AlleleB_ProbeSeq), original genomic sequence used for probe design after bisulfite conversion (SourceSeq), build of the consensus reference genome (mouse, mus musculus) (Genome_Build), forward or reverse strand (Strand), top or bottom strand (Strand_TB), converted or opposite (Strand_CO), functional change of a probe due to production error of the array; typically, false indicates regular functionality (MFG_Change_Flagged), location of the methylation change on the transcription start site (TSS) (tss_body), location of the methyation change 200 bps around TSS (tss_200), location of the methylation change 1500 bp around TSS (tss_1500).

Supplementary Table S4: Table depicts all 19 protein-coding genes upregulated after 24 h ephrinA5-Fc treatment and with putative triplex target DNA sites (TTS) for *Snhg15* (RNA-seq; Pensold et al. 2021).

Supplementary Methods:

Survival Analysis

The survival analysis was implemented in R. It was based on clinical data and gene expression counts from tumor samples of lower grade glioma patients downloaded from BioPortal (http://www.cbioportal.org/study/clinicalData?id=lgg_tcga) and The Cancer Genome Atlas (TCGA), respectively. To download the gene expression counts, we applied the R package TCGAbiolinks setting the parameters for GDCquery as follows: project="TCGA-LGG", data.category="Transcriptome Profiling", data.type="Gene Expression Quantification", workflow.type="HTSeq – Counts" and sample.type=c("Primary solid Tumor", "Recurrent Solid Tumor"). The raw gene counts were normalized by applying DESeq2::varianceStabilizingTransformation(). Afterwards, the patients were divided into two groups (high expression, low expression) based on whether their NCAM1 expression level is above or below the median NCAM1 expression level among all patients. Using survival::Surv() and survival::survfit() while setting the time parameter to the survived months and the event parameter to the patients' vital status from the clinical data a Kaplan-Meier curve object was created. It was plotted with survminer:: ggsurvplot() setting risk.table=TRUE. If not indicated otherwise, default parameters have been passed to the applied R functions.

Supplementary Figures:

Supplementary Figure 1

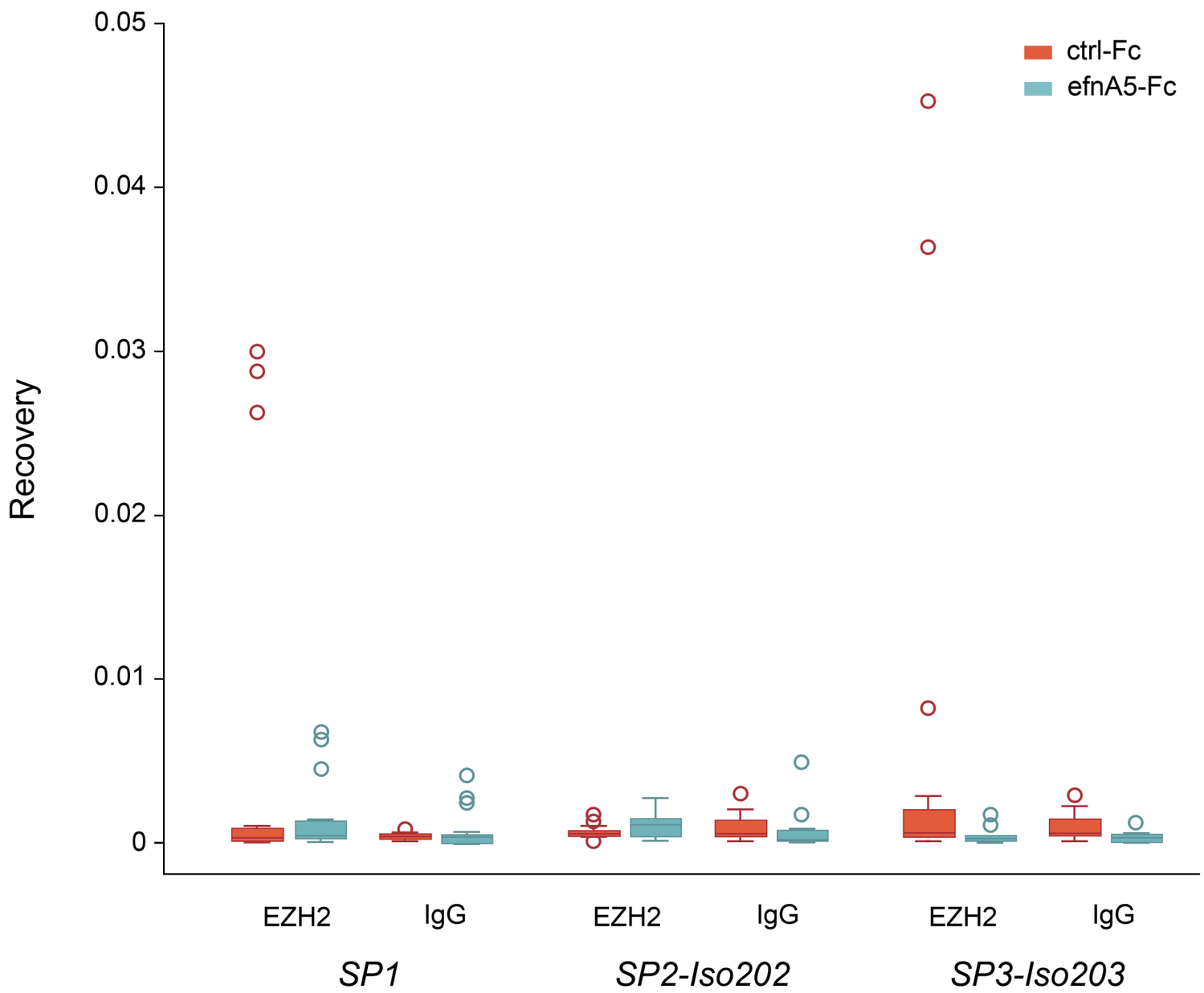

Supplementary Figure 2:

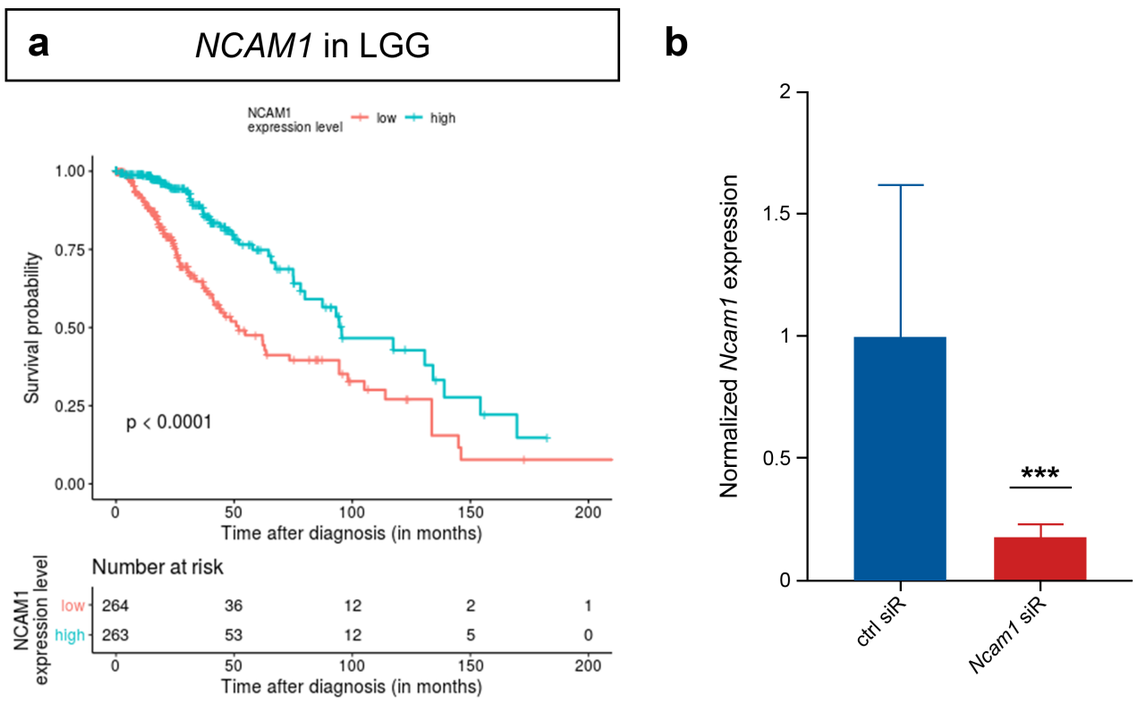

Supplementary Figure 3:

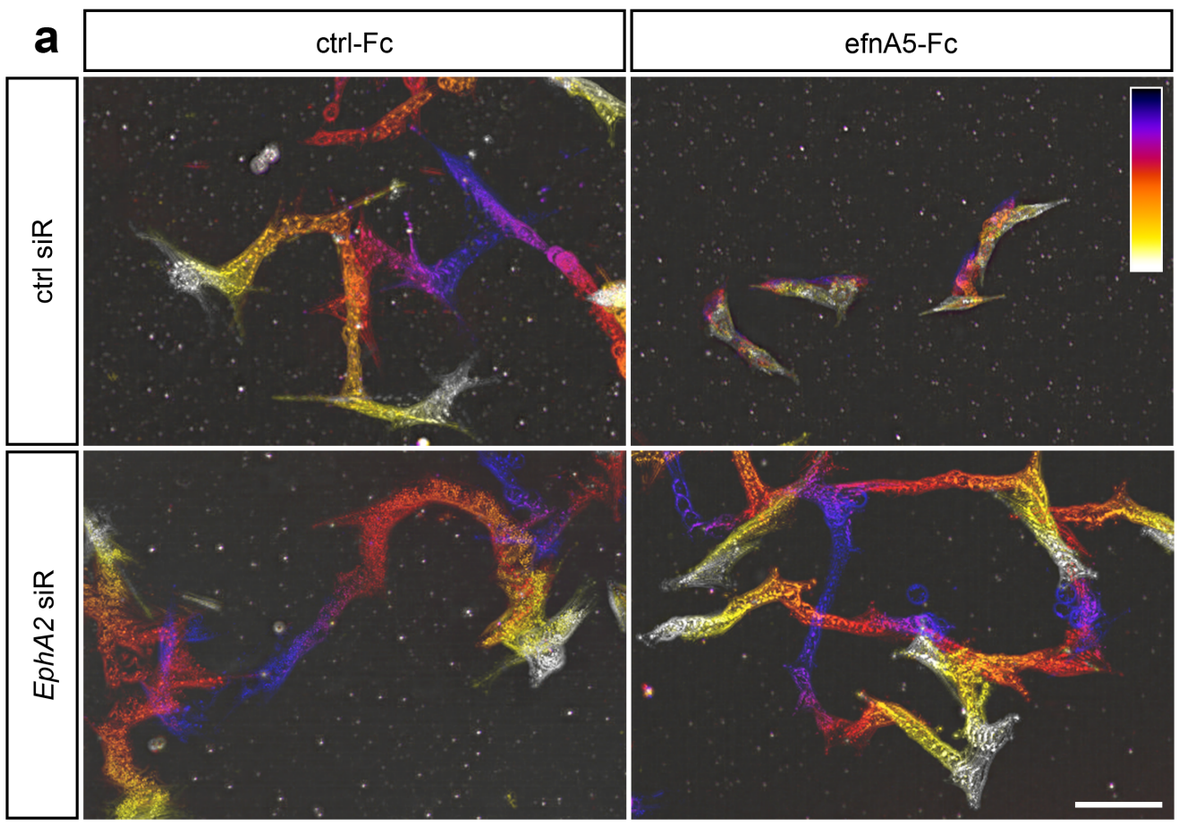

Supplementary Figure S4:

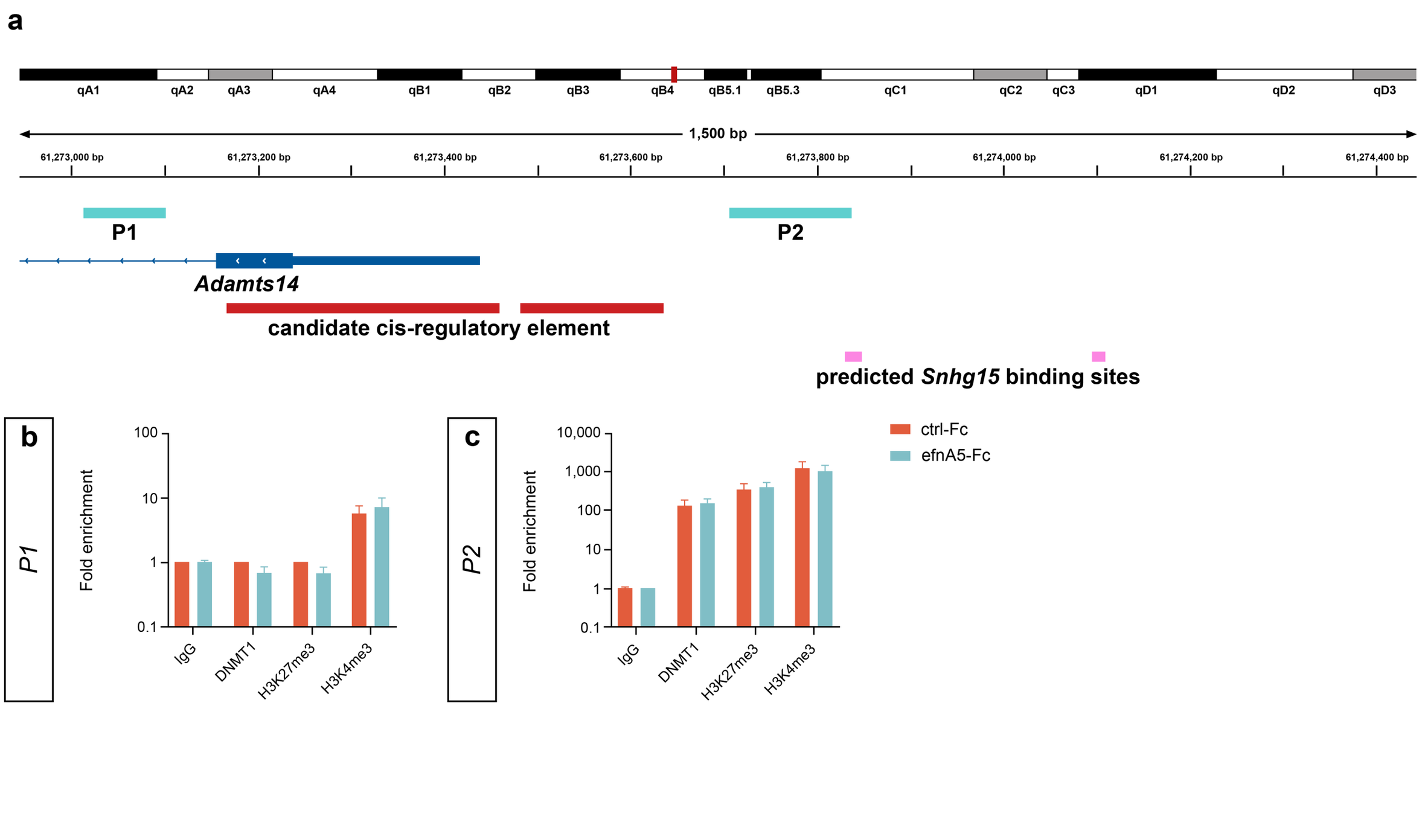

Supplementary Figure S5:

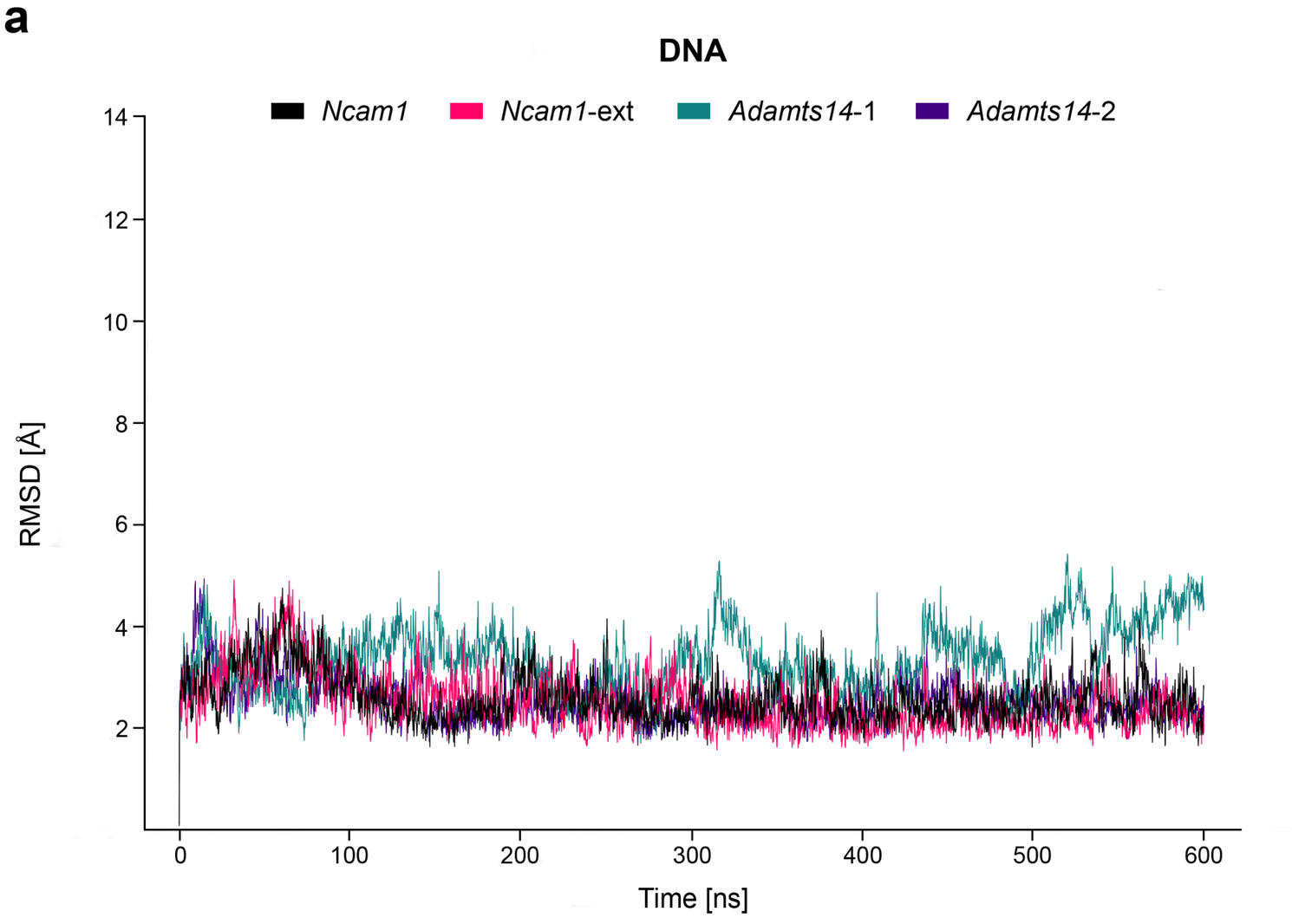

Supplementary Figure S6:

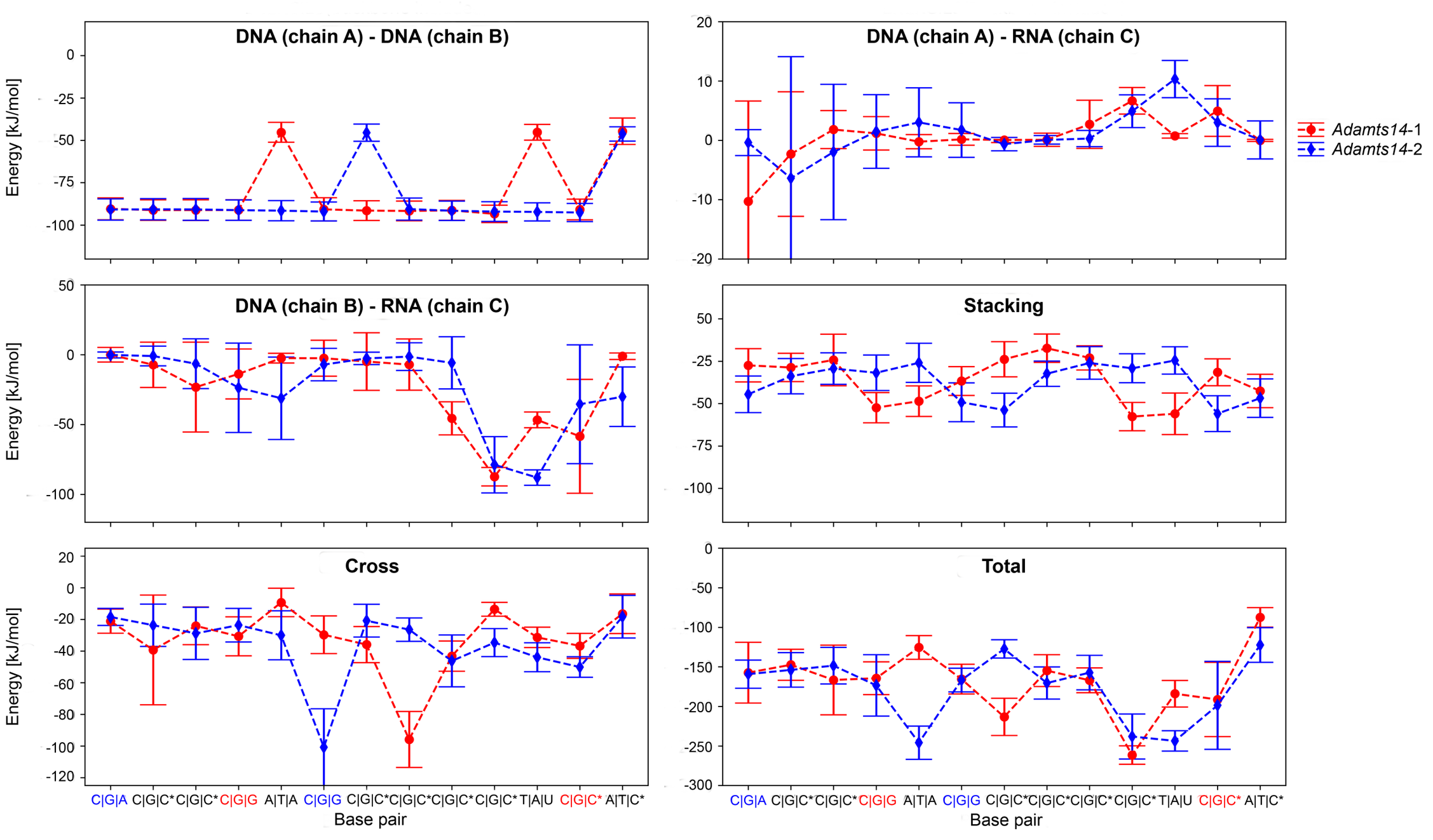

Supplementary Figure S7:

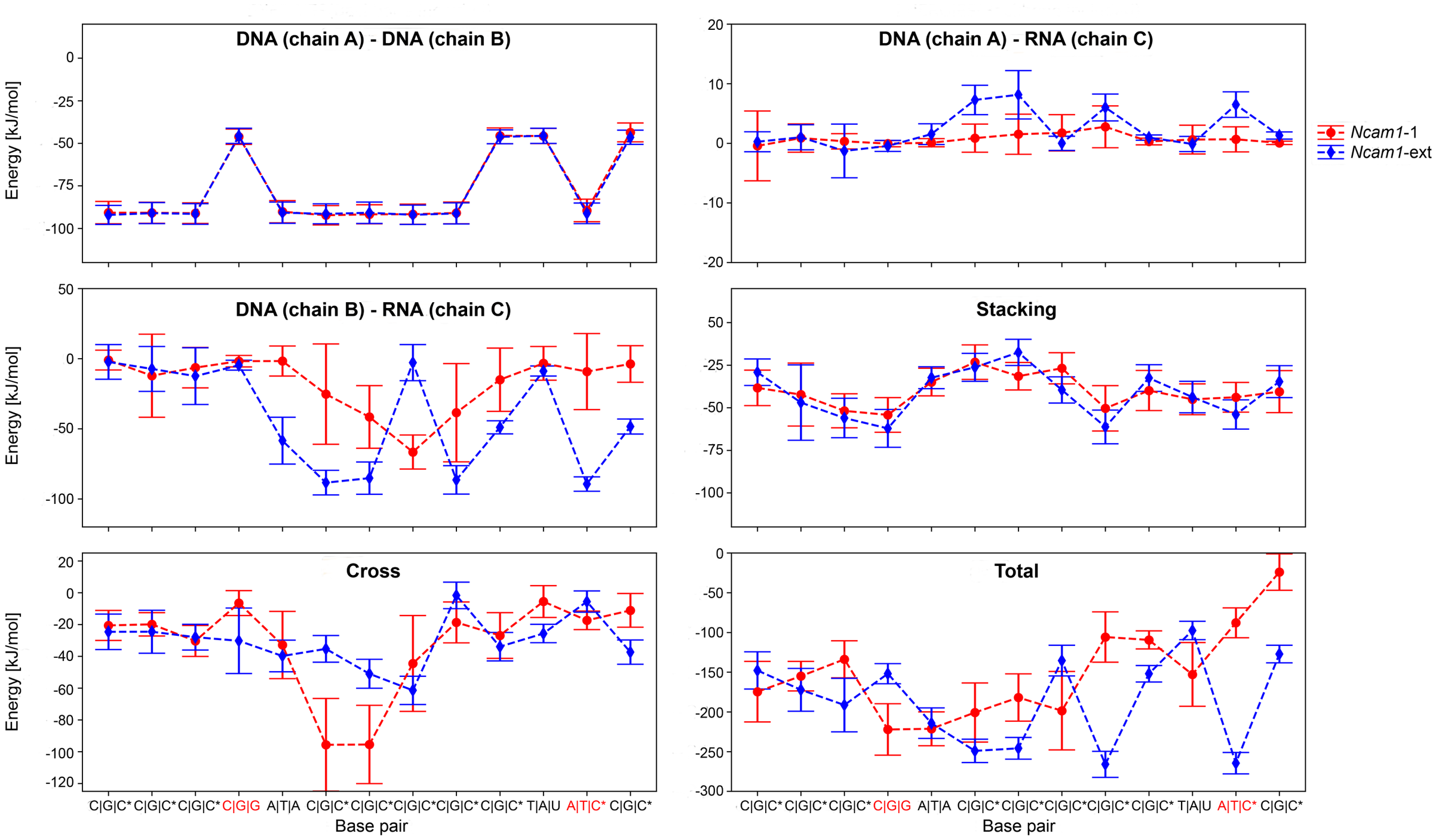

Supplementary Figure S8:

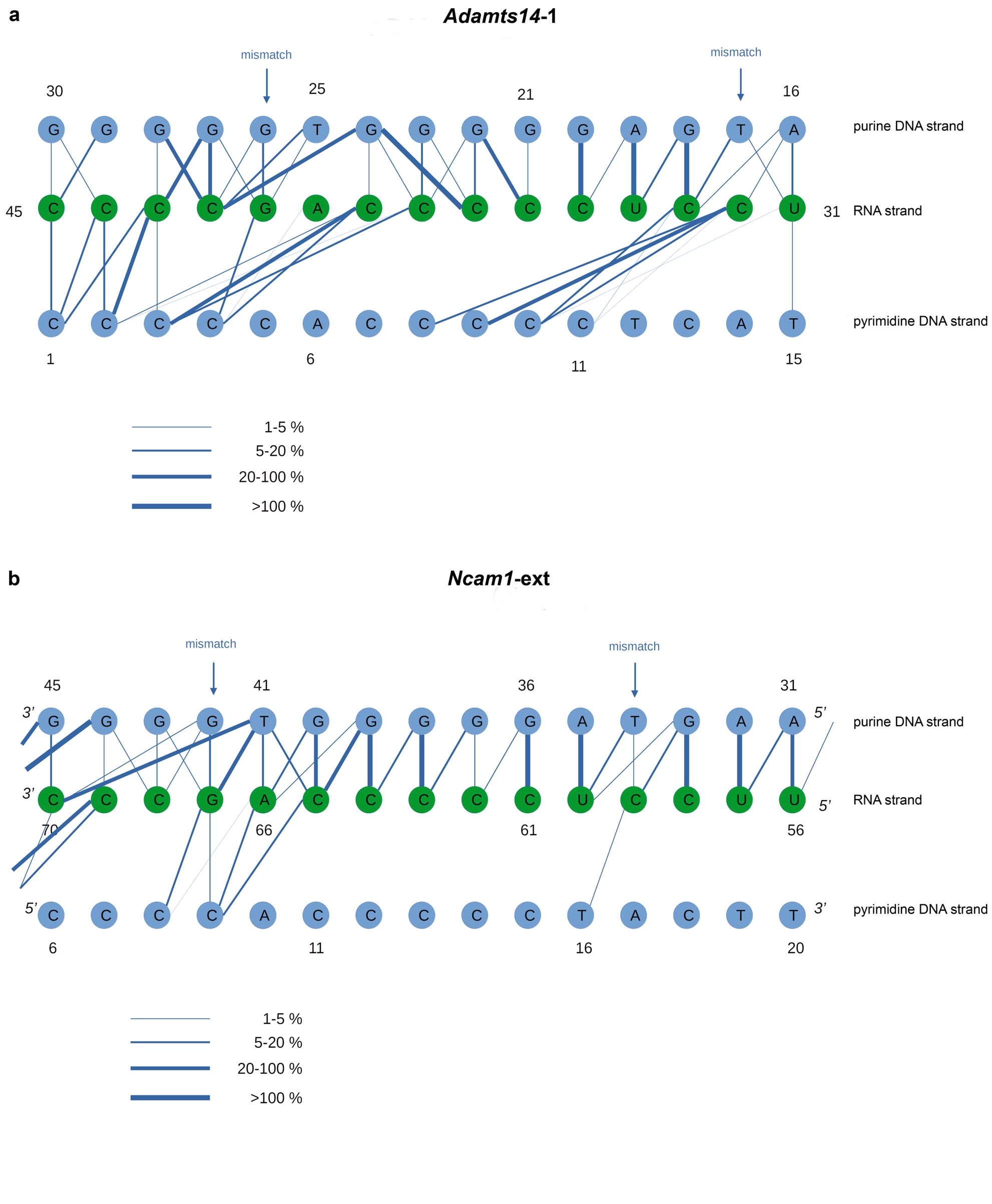

Supplementary Table S1:

Target	Descriptor	Sequence	Product size [bp]
Adamts14 (DNA)	*P1*	F: AAAGCTAAGCAACTCAACCCAC R: AGAGTGGCTCCTGGATGCAG	90
	P2	F: CATTGAATTTTGAAGGCGCAGATTG R: CTCATATCGTTGTGACCTGACAG	132
Atp5bp (mRNA)		F: TGTGATTACCCCAGAGACCT R: TGCTCGACTGCTTTACTTCTTC	149
EphA2 (mRNA)		F: GTGTGCAAGGTGTCCGATTT R: AACTTGCGGTAGGAAATGGC	128
Ncam1 (DNA)	*P1*	F: TTATTCGGGGCGGGGAAGAC R: CTAGAGGTGTTTGTCAAGCTTCGAG	137
	P2	F: GACAATTAACAGACCCGATGTAGAT R: ACTAAGGATCTCATCTGGACTTTGT	98
	P3	F: TTTTCCTTCATTCACGTCTTTGGAG R: GTGTCCACAACTTTGAAAATCGAAC	129
Ncam1 (mRNA)		F: GGTGACCCCTGATTCAGAAA R: GGATGGAGAAGACGGTGTGT	118
Snhg15 (lncRNA)	*SP1*	F: GCCCTCACCTTATCTTCCGT R: AGCTCAGCCATCTCTACCTG	78
	SP2	F: AGCCTGTGTTCTTTTCTGGAG R: AGGAAGAGTCAGTGAGCCAA	145
	SP3	F: CTACAGCGTGGAAGGGATGA R: TCCCAGTCCCCAGAAGTCTA	143

Supplementary Table S2:

Name (PDB code)	Description	Sequence
Adamts14-1	DNA - DNA | RNA	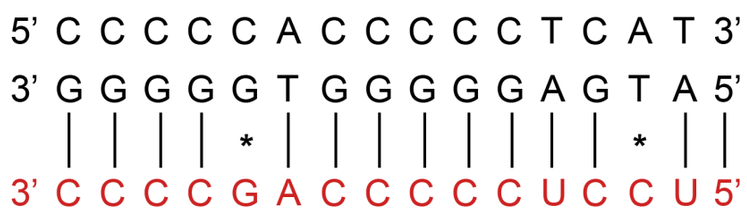
Adamts14-2	DNA - DNA | RNA	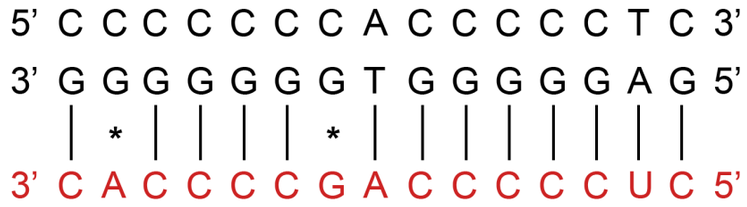
Ncam1	DNA - DNA | RNA	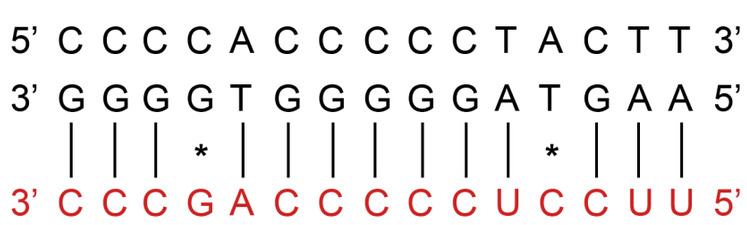
Ncam1-ext	DNA - DNA | RNA	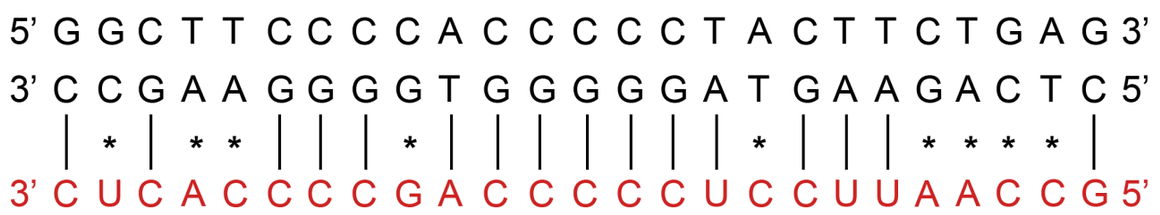

Supplementary Table S4:

Promoter	Gene	TTSs Count	TTS Coverage
chr4:53159894-53160895	*Abca1*	31	0.31
chr17:43800350-43801351	*Rcan2*	43	0.11
chr3:89214179-89215180	*Thbs3*	49	0.08
chr9:62537043-62538044	*Coro2b*	68	0.07
chr9:13296956-13297957	*Maml2*	15	0.12
chr15:83088505-83089506	*Sehrl*	15	0.07
chr3:52105075-52106076	*Maml3*	14	0.07
chr18:79109390-79110391	*Setbp1*	8	0.07
chr8:82862355-82863356	*Rnf150*	5	0.048
chr4:130046839-130047840	*Col16a1*	8	0.042
chr4:114405723-114406724	*Trabd2b*	5	0.044
chr7:98488282-98489283	*Lrrc32*	3	0.045
chr10:61273437-61274438	*Adamts14*	4	0.032
chr18:44812181-44813182	*Mcc*	2	0.031
chr19:31765032-31766033	*Prkg1*	2	0.031
chr2:173276532-173277533	*Pmepa1*	1	0.015
chr9:49798924-49799925	*Ncam1*	76	0.23
chr10:8518824-8519825	*Ust*	46	0.15
chr18:33464028-33465029	*Nrep*	83	0.09